In situ powder neutron diffraction of cation partitioning vs. pressure in $Mg_{0.94}Al_{2.04}O_4$ synthetic spinel

ALESSANDRO PAVESE,[1,*] GILBERTO ARTIOLI,[1] AND STEVE HULL[2]

[1]Dipartimento di Scienze della Terra, Università di Milano, I-20133 Milano, Italy
[2]Rutherford Appleton Laboratory, ISIS Facility, Chilton-Didcot, Oxfordshire, OX11 0QX, U.K.

ABSTRACT

Powder neutron diffraction [ISIS Facility (U.K.), POLARIS diffractometer] was used to investigate the effect of elevated pressure on cation partitioning in synthetic $Mg_{0.94}Al_{2.04}O_4$ spinel. The distributions of Mg, Al, and vacancies were studied as a function of pressure, by refinement of the T- and M-site scattering lengths, and determination of the cation partitioning through numerical minimization methods. The partially disordered Mg/Al distribution, which results from the synthesis process, show an increase in ordering between 6 and 18 kbar, where Mg and Al order to the T- and M-sites, respectively. Pressure effectively tends to stabilize MgAl-spinels with a "normal structure," and this behavior is supported by numerical simulations based on classical electrostatic calculations.

INTRODUCTION

Spinels are ternary oxides, space group $Fd\bar{3}m$, whose elementary cell contains 32 O atoms in cubic close packing arrangement, 16 octahedrally (M) and 13 tetrahedrally (T) coordinated sites, which can host various cations (e.g., Fe, Al, Mg, and Mn). Ideal AB_2O_4 end-members may in principle have two possible cation distributions, leading either to the "normal structure" (NS), wherein A- and B-cations are tetrahedrally and octahedrally coordinated, or to the "inverse structure" (IS), wherein half of the B-cations enter T-sites, left empty by the A-cation migration to the M-sites. Intermediate cation distributions usually occur in natural spinels.

Mg-Al-Fe-rich spinels are considered to be important constituents of the upper mantle of the Earth and the knowledge of their crystal-chemical behavior at extreme conditions is essential for the interpretation of many petrological processes (Sack and Ghiorso 1991; Gasparik and Newton 1984). In particular, cation partitioning in spinels is closely related to pressure and temperature, as both the energetics and the configurational entropy are dependent on the atomic distribution over T- and M-sites. Moreover, spinels are also used for technological applications, e.g., as refractory materials, and their physical properties are well known to be partly related to the cation distribution. Because of the above considerations, the research activity concerning spinels is lively, and mainly directed to the definition of the mechanisms governing cation partitioning [see Della Giusta et al. (1996) for a survey on the subject].

Order-disorder (OD) reactions involving tetrahedral and octahedral cation diffusion induced by temperature have been widely studied by spectroscopic and diffraction techniques, mostly using samples after thermal quench (Wood et al. 1986; O'Neill et al. 1991; Millard et al. 1992; O'Neill 1992; O'Neill et al. 1992; Larsson 1995; Della Giusta et al. 1996; Menegazzo et al. 1997), and just in a few cases by in situ measurements (Yamanaka and Takeuchi 1983; Peterson et al. 1985; Pavese et al. 1998). Hazen and Navrotsky (1996) speculated on how the pressure affects OD-reactions in condensed matter, and pointed out that the baric component provides an important, though often unduly neglected, contribution in driving such phenomena. Pressure is generally regarded as an obstacle to processes based on thermally activated intracrystalline diffusion, because the compressional forces reduce the interatomic voids. However, to achieve the structure having the minimum Gibbs energy and stable at given P and T, cation rearrangement driven by pressure cannot a priori be discarded.

A particularly interesting case is that of spinel, i.e., $MgAl_2O_4$, that ideally at ambient condition has a NS. Taking into account the fact that the lattice parameter of spinel is expressable as a function of T-O and M-O bond lengths, a straightforward calculation, relying on ionic radii (Menegazzo et al. 1997), shows the IS volume to be 1.3% smaller than the NS volume. This observation indicates that (1) there is a well known discrepancy in $MgAl_2O_4$ between the observed cation distribution and the predicted one derived from basic crystal chemical principles; (2) it is not unreasonable to expect that, starting from some partially inverted Mg/Al-partitioning, the action of pressure might somehow favor a rearrangement which, a priori, we are not able to predict from simple geometrical arguments. A more complete interpretation ought to include at least the energetics of the system and the compressional behavior of the interatomic bonds.

Some early high-pressure studies on $MgAl_2O_4$ were carried out by Liu (1975, 1978, 1980); however, just one crystallographic investigation of the behavior of normal spinel under P has been published so far, from Finger et al. (1986) by means of single-crystal X-ray diffraction up to 40 kbar. No investiga-

*E-mail: pavese@p8000.terra.unimi.it

tion aimed at clarifying the effect, if any, of pressure on cation partitioning in spinel-like materials is available in literature.

This fact led us to carry out a high pressure study of the crystal-chemical behavior of $MgAl_2O_4$ by means of neutron powder diffraction. The neutron scattering length contrast between Al and Mg makes it possible to unambiguously separate the contributions to diffraction signals from these chemical species. The large amount of material required for neutron scattering studies, and the intention to start from a partially disordered Mg/Al distribution, motivated the use of synthetic $MgAl_2O_4$.

EXPERIMENTAL METHODS

The synthetic sample was obtained by heating a stoichiometric mixture of reagent grades MgO, and $A1_20_3$ at 1600 °C, for approximately 10 h. The chemical composition was determined by averaging the results of 30 chemical analyses obtained by means of an ARL SEMQ electron probe microanalyzer. The resulting unit formula, $Mg_{0.94}A1_{2.04}0_4$, indicates the presence of about 0.02 vacant sites p.f.u., in full agreement with the value inferred by the relationship from Lucchesi and Della Giusta (1994), that links the vacancy content to the cell edge [a = 8.0704(1) Å].

The diffraction measurements were performed at ISIS Facility (U.K.), by using the time of flight (TOF) technique, on the high intensity powder diffractometer POLARIS (Hull et al. 1992; Smith and Hull 1997). This instrument has three collection banks, placed at 28°, 90°, and 140° with respect to the incident beam, and equipped with ZnS scintillator detector arrays. High pressure was achieved by means of a standard Paris-Edinburgh cell (Besson et al. 1992), which allows recording of patterns at the 90° bank ($\delta d/d \approx 10^{-3}$); NaCl was used as an internal P-calibrant, and pressure was estimated using the equation of state from Birch (1986). The sample, pre-compressed into a 80 mm^3 volume pellet, was positioned in between the tungsten carbide clamps, and surrounded by a toroidal gasket to prevent lateral leakage of material. The incoming beam enters the PE-cell along the thrust axis, and the diffracted neutrons are collected over a 12° in 2θ angle, i.e., at 90 ± 6°; reductions of the effective diffraction cone occur with increasing pressure, as a consequence of the experimental geometry.

A first set of data was recorded at ten P-values to determine the EOS of spinel and the pressure calibration curve, for estimating P in the next experiments without internal standard; this set of measurements took some 24 h. A pellet prepared with equal amounts of NaCl and spinel was used. Six more powder patterns were then recorded at increasing pressure values, from a one-phase spinel pellet, to investigate the crystal-chemical features of the sample at HP; in this case, a larger collection time was adopted, 72 h in total, to achieve counting statistics that enable reliable study of the cation partitioning. One powder pattern was recorded at room conditions, outside the PE-cell, to be used later for reference. Absorption effects, due to the pressure cell and affecting the diffraction profile intensities, were partially corrected by laboratory supplied routines. A more appropriate empirical correction for aberrations due to the high-pressure device was derived by comparing the structural parameters (cell edge, oxygen u-coordinate, ADPs = Atomic Displacement Parameters) obtained from the refinement of data collected at room pressure with and without the PE-cell. In Figures 1a and 1b the profiles at ambient conditions and at 38 kbar, recorded at the 90° bank, are shown. In Figure 1b, the peak about 1.87 Å, not matching any of the spinel reflections, is due to the tungsten carbide clamps, and it has been ruled out during the profile analyses.

The collected patterns were analyzed by the Rietveld method, using the GSAS package (Larson and Von Dreele 1987). A pseudo Voigt convoluted with a back-to-back exponential function was used for modeling the diffraction profiles; the Lorentzian (γ) and Gaussian (σ) components of the FWHM were parameterized as follows $\gamma = \gamma_0 + \gamma_1 d + \gamma_2 d^2$ and $\sigma^2 = \sigma_0^2 + \sigma_1^2 d^2 + \sigma_2^2 d^4$. σ_1 and γ_2 terms, related to the strain and to the crystallite size respectively, were allowed to vary during the reference refinement, whereas the latter was kept fixed in the treatments of data at high pressure. The scattering lengths of O, Mg, and Al from the GSAS database (0.5805, 0.5375, 0.345 10^{-12} cm, respectively) were used for the refinements.

DATA TREATMENT

The analysis of the T- and M-site occupancies was carried out by a two-step procedure. First, the octahedral and tetrahedral site scattering lengths (b_T and b_M) were refined, under the

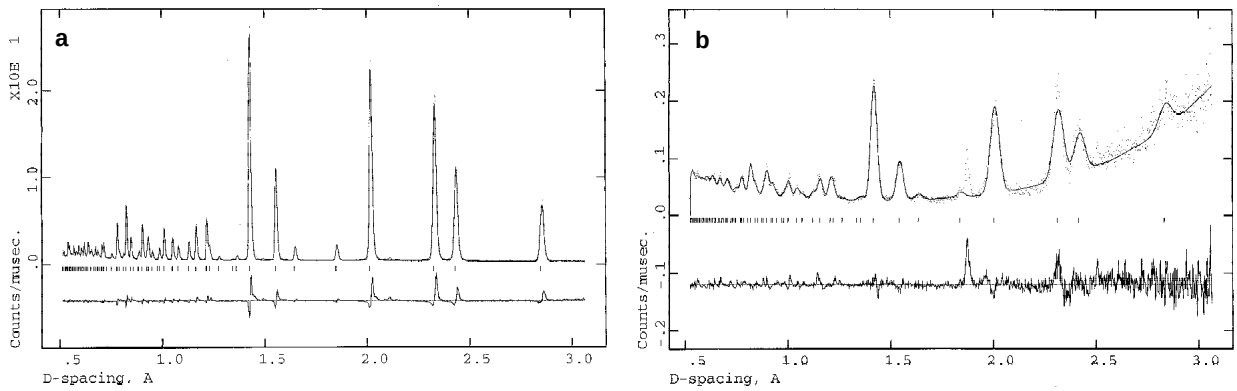

FIGURE 1. Observed (top spectrum), calculated (middle, short lines) and residual (bottom curve) powder neutron diffraction patterns at ambient condition, outside the PE-cell **(a)**, and at 38 kbar **(b)**. Dots are actual data points.

constraint of conservation of the total scattering length per unit cell, that results from the invariance of the chemical composition. This requirement is fulfilled when

$$0 = \delta b_T + 2 \times \delta b_M \quad (1)$$

where $\delta b_x s$ are the shifts of b_T and b_M during the least squares minimization cycles.

Table 1 lists the structural parameters obtained from the Rietveld refinements of the data sets collected over the 0–40 kbar range. The behavior of the ADPs is to be discussed: U(T) increases whereas U(M) significantly decreases, with pressure. The thermal parameters play an important role in the determination of cation distributions, that are well known to correlate with scale factor and ADPs. This factor is even more severe in high-pressure experiments, where the absorption due to the pressure cell further degrades the quality of the diffraction signals, the effect of which generally increases with pressure.

Two refinement schemes were tested to limit, as much as possible, the ambiguities arising from factors affecting the ADPs: In one (C-mode) the variations of the tetrahedral and octahedral ADPs were restrained so as to maintain U(T) = U(M), whereas in the other (UN-mode) no constraint was used. In principle, no theoretical reason exists to support the C-scheme, save that U(T) and U(M) are within 2σ apart, according to the refinement from the reference data collection.

In the second step of the analysis, the Mg, Al, and vacancies partitioning was extracted using the minimization technique of Pavese et al. (1999), based on a combination of the simplex and Newton-Raphson methods, and implemented as an extension of the MINUIT code (James and Roos 1975). The aim of the computational technique consists in finding the cation distribution that minimizes the target function defined as

$$\Phi = \sum_j \left(A_{\text{obs},j} - A_{\text{theo},j}\right)^2 \times W_j \quad (2)$$

where $A_{\text{obs},j}$ are experimentally measured quantities (chemical composition, site-scattering lengths, full occupancy requirements for M- and T-sites) and $A_{\text{theo},j}$ the corresponding calculated values; W_j is a weighting factor, established on the basis of the error affecting the jth-observation. $A_{\text{theo},j}$ are expressible as linear combination of the site population coefficients, i.e., Y_{Al}, Y_{Mg}, $Y_{\square}$, X_{Al}, X_{Mg}, $X_{\square}$, where the subscript indicates the chemical species or vacancy $\square$ involved, and X and Y refer to T- and M-sites, respectively. The six {X,Y} terms require at least as many constraining equations to be determined. In our case, the T- and M-site scattering lengths, the Mg and Al content, and the condition of individual site full occupancy, provide six constraints, prescribing one solution to exist, which minimizes Equation 2.

Using this treatment, we were able to select the refinement strategy providing the most sound results. Whereas the C-scheme yielded site scattering lengths inconsistent with the overall chemical composition and the site full-occupancy requirements, the UN-refinement mode led to b_T and b_M values fairly matching the bulk crystal-chemistry of the compound.

In the framework of the UN-scheme, we also tested the rather unlikely occurrence of anisotropic broadening. If not taken into account this might cause profile mismatches reflecting over ADPs, which would suffer unsound values to arrange the heights of the calculated peaks for better fitting experimental profiles, unduly broad/sharp with respect to the theoretical ones. These tests, however, allowed us to discard anisotropic broadening as a possible cause of the anomalous behavior of the ADPs.

Finally, to check the effects of the correlations between background-ADPs-site scattering lengths, we performed some refinements by fixing the background coefficients, previously determined by means of several profile points judiciously selected where no sample peaks are present. The results achieved confirmed those obtained with the unconstrained background treatment.

Having explored and discarded any reasonable effect that, if neglected, causes the anomalous behavior of the ADPs, we conclude that the trend exhibited by U(T) and U(M) can to be ascribed to the absorption of the high-pressure cell, because this effect was not totally corrected for by the standard procedure mentioned above. Although in principle all atoms ought to show comparable anomalies in the ADPs, the observed site-selectiveness of the absorption is most likely due to the fact that, in spinels, some reflections are dominated by single-site scattering. Consequently, in the TOF-technique, which relies on the λ-dispersion mode, peak-locations are related to wavelength, and therefore specific classes of reflections may selectively suffer absorption.

Moreover, the T-cation sites have been proved to be often affected by local clustering effects, as a consequence of different second neighbor shells surrounding the tetrahedrally and octahedrally coordinated cations, and that cause energetically non-equivalent M- and/or T-sites, as demonstrated by Mössbauer spectroscopy (Carbonin et at. 1996). These effects may influence the anomalous behavior of the T- and M-site ADPs (Pavese et a1. 1999).

The normalization with respect to the results attained from the reference data collection renders the refined site scattering lengths independent of the behavior of the ADPs, i.e., of the effects due to absorption. A further support to this conclusion

TABLE 1. Lattice parameter, oxygen u-coordinate, and ADPs of spinel

P (kbar)	a (Å)	u(O) (Å² × 100)	U(O) (Å² × 100)	U(T) (Å² × 100)	U(M) (Å² × 100)	b_T (10^{-12} cm)	b_M (10^{-12} cm)	wR_p —
0.0	8.0704(1)	0.26171(7)	0.68(4)	0.40(7)	0.41(5)	0.493(3)	0.358(6)	9.1
0.7(1)	8.0694(1)	0.26174(6)	0.73(4)	0.47(7)	0.45(5)	0.497(3)	0.356(6)	9.5
6.3(1)	8.0616(2)	0.26146(8)	0.85(5)	0.67(9)	0.49(6)	0.495(3)	0.357(6)	9.5
18.2(1)	8.0452(4)	0.26139(9)	1.00(6)	1.5(1)	0.16(7)	0.522(3)	0.343(6)	8.9
26.5(1)	8.0339(5)	0.26108(11)	1.10(6)	1.8(1)	0.02(8)	0.521(3)	0.344(6)	8.3
38.1(2)	8.0187(5)	0.26079(11)	1.19(6)	2.0(1)	0.20(8)	0.521(3)	0.344(6)	7.5

Notes: $wR_p = \sqrt{\sum \left(I_{\text{obs}} - I_{\text{calc}}\right)^2 w \,/\, I_{\text{obs}}^2 w} \times 100$.

is that the site-scattering lengths show an evident change between 6 and 18 kbar, and their values are constant above or below that *P*-interval; otherwise, in the case of residual effects due to absorption, one would expect a drift of b_T and b_M, as a function of *P*.

RESULTS AND DISCUSSION

Cation partitioning

Fitting the dependence of the unit-cell volume *V* of spinel on pressure to a Birch-Murnaghan (1986) equation of state yields K_0 = 190(±2) GPa, assuming K_0' = 4, and K_0 = 195(±7) GPa K_0' = 2.2(±2), if the bulk modulus and its first pressure derivative, at *P* = 0, are allowed to vary (Fig. 2). These results are in good agreement with those previously obtained by Wang and Simmons (1972), K_0 = 195 GPa, and by Finger et al. (1986), K_0 = 194(±6) GPa, though the value of K_0 presently attained is slightly lower than that of the most recent determination after Askarpour et al. (1993), K_0 = 198(±8) GPa. The observed small discrepancies, which never exceed 3%, are ascribable to the presence in the synthetic samples of vacancies and of slightly different cation ordering over tetrahedral and octahedral sites, that can influence some of the physical properties of spinels (Viertel and Seifert 1979; Askarpour et al. 1993).

Abrupt changes of b_M and b_T are seen with increasing *P* from 6.3 to 18.2 kbar (Table 1), suggesting that an order-disorder reaction has taken place. One interpretation of the cation partitioning is given in Table 2; the last digit corresponds to the magnitude of the numerical oscillations at convergence of the minimization process. The significance of the partitioning coefficients can be roughly estimated based on the uncertainties over the chemical composition and the site-scattering lengths determined from Rietveld refinements, and it results approximately 0.015. At ambient condition, our sample has a partially disordered Al-Mg distribution, whereas the vacancies (□) are fully segregated into the T-sites. This tendency of □ is in agreement with that determined by Pavese et a1. (1998) by powder neutron diffraction vs. temperature, on synthetic Mg-Al-Fe spinel. Increasing pressure causes Mg-atoms to order into the T-site, whereas Al exhibits preference for the sixfold coordination; vacancies, are limited to the tetrahedral site at low pressure, and they redistribute over both M- and T-sites at high pressure. Evidently pressure promotes the stability of a normal-like structure, with a nearly equi-partitioning of vacancies between tetrahedral and octahedral sites. In principle an "inverse" structure would appear more appropriate at high pressure on account of its smaller cell volume with respect to NS values, according to calculations based on the conventional ionic radii, (Hazen and Navrotsky 1963; Della Giusta and Ottonello 1993). However, this notion has to be revised in view of (1) the linear relationship between ionic radii and bond been proved fully valid under ambient conditions and in the lengths in spinel has been proved fully valid under ambient conditions and in the case of natural samples, but does not hold for our synthetic Mg-Al-spinel studied at high pressure; (2) the purely geometrical approach totally disregards the bonding energetics. The static energy plays a crucial role in driving any high-pressure process, and neglecting it can lead to erroneous interpretations.

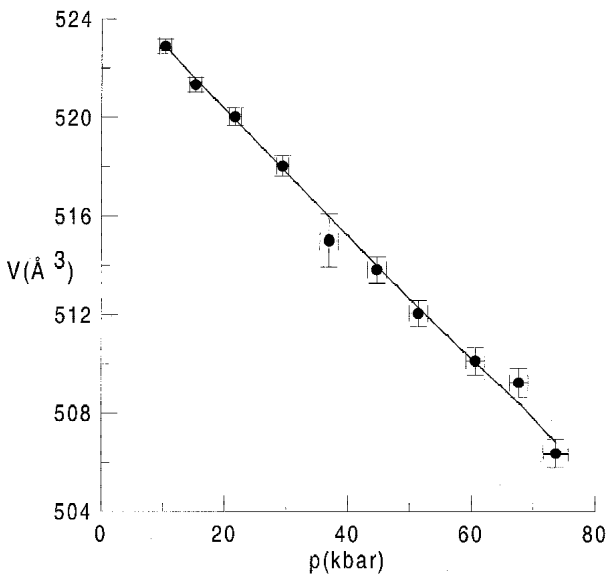

FIGURE 2. Cell volume (Å^3) vs. pressure (kbar).

Bond lengths and angles

The interatomic bond lengths, angles and polyhedral volumes, are consistent with the conclusions thus far achieved concerning the cation partitioning. However, because most of these structure parameters exhibit large e.s.d's, the considerations reported below rely on their trends, rather than on their absolute values.

The octahedral cation-oxygen bond lengths exhibit an abrupt change occurring at the OD-reaction pressure (Fig. 3a), whereas the tetrahedral bond length shows a substantial but smooth decrease with *P* (Fig. 3b). We believe this behavior qualitatively reflects changes in site populations: (1) Initially, <T-O> undergoes compression since vacancies occupy the T-sites and soften the bond, whereas the M-sites is fully occupied by Mg and Al cations and <M-O> distance behaves more rigidly; (2) above the OD-transition pressure, the T-sites become more Mg-rich, at the expense of Al and vacancies, but suffer little change of their site-compressibility because, though the Al-O bond is expect to be more rigid than Mg-O, this effect is partly balanced by the migration from fourfold to sixfold coordination of approximately half of the vacancies; (3) the <M-O> bond is stiff at ambient pressure, because the site is fully occupied by Mg and Al, and collapses between 6 and 18 kbar, and remains nearly constant with increasing *P*. This behavior could result from the replacement of Mg with Al, which is expected to favor shorter and less

TABLE 2. Cation partitioning determined as reported in the text

P (kbar)	X_{Mg}	X_{Al}	Y_{Mg}	Y_{Al}	$X_{□}$	$Y_{□}$
0.0	0.8035	0.1760	0.0675	0.9324	0.0204	0.0000
0.7(1)	0.8243	0.1552	0.0572	0.9428	0.0205	0.0000
6.3(1)	0.8139	0.1657	0.0624	0.9376	0.0204	0.0000
18.2(1)	0.9387	0.0500	0.0000	0.9954	0.0113	0.0046
26.5(1)	0.9386	0.0558	0.0007	0.9916	0.0097	0.0048
38.1(2)	0.9387	0.0459	0.0000	0.9975	0.0155	0.0025

Notes: X and *Y* refer to the tetrahedral and octahedral sites, respectively. The subscripts indicate the corresponding chemical species; □ means vacancies.

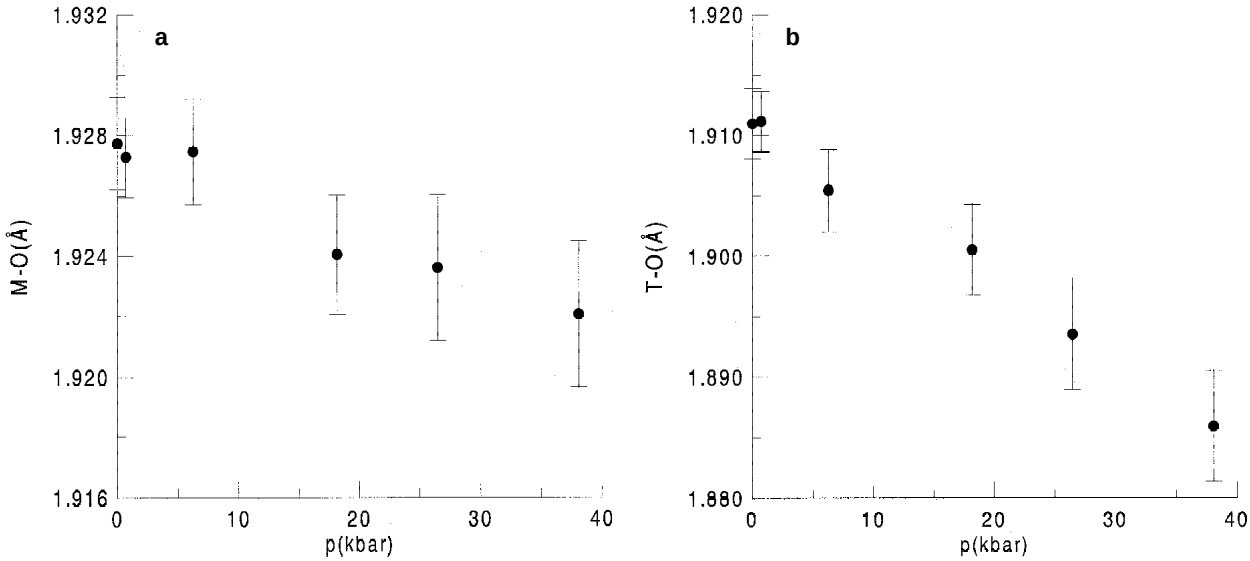

FIGURE 3. Octahedral **(a)** and tetrahedral **(b)** cation-oxygen bond lengths (Å) vs. pressure (kbar).

compressible bonds than magnesium does, owing the smaller cation size of aluminum. Moreover, although some octahedral vacancies are created, they are less effective in affecting the compressional features of the M-O bond than in the case of the T-O bond, given that vacancies are twice as likely to occur at T-sites than at M-sites, owing to the site-multiplicity.

Information on the structural behavior of the sample under compression can also be obtained from the trend vs. *P* of the T-O-M angle (α), of the shared (*ose*) and unshared (*oue*) octahedral edges, of the tetrahedral edge (*te*), and of the polyhedral volumes. Their values are not given in the tables, but are readily calculated from the oxygen *u*-coordinate and the cell edge (Nakagiri et al. 1986). These structural parameters (generically labeled *W* in the expression below) are discussed using the concepts of "maximum relative variation" and of "rate of variation," defined as:

$$MRV(W) = \frac{W_P - W_0}{P} \times \frac{1}{W_0} \quad (3)$$

and

$$RV(W) = \frac{W_P - W_0}{P} \quad (4)$$

where *P* and 0 refer to the highest pressure we achieved, and to the room conditions, respectively. Definition 3 is close to that of standard bond compressibility, and identical with it at $P = 0$ if the response of the bond length to pressure is linear. In the present case, the Equations 3 and 4 simply provide a rough estimate of the behavior of *W* vs. *P*, which can be compared with the previous results from Finger et al. (1986). MRV cannot be related to the usual compressibility concept, as the trends of the structural quantities reported in the figures lack continuity. In the following discussion, MRVs are multiplied by 10^6.

Marked discontinuities are apparent in the curves of α (Fig. 4) and of *ose* (Fig. 5a) vs. pressure, in agreement with the occurrence of the assumed OD-reaction The *oue* curve displays a rather smooth trend with pressure (Fig. 5b), and the *te* points exhibit a much smaller discontinuity (Fig. 6). The *u*-coordinate of oxygen, not plotted for the sake of brevity, evidences, as well, the presence of a discontinuity vs. pressure, in contrast with Figure l from Finger et al. (1986), wherein the smooth trend shown suggests no OD-reaction to occur under pressure and, in the light of the preceding discussion, a cation arrangement according to the normal structure, or at least very close to, is likely to be in their sample.

The change in the α-angle with pressure occurs about a rate of 0.009 deg/kbar (MRV = 71). The corresponding value obtained by Finger et al. (1986) is 0.005 deg/kbar, possibly indicating a vacancy-enhanced disposition to T-O-M bond bending in our synthetic MgAl-spinel. In fact, the absence of atoms at

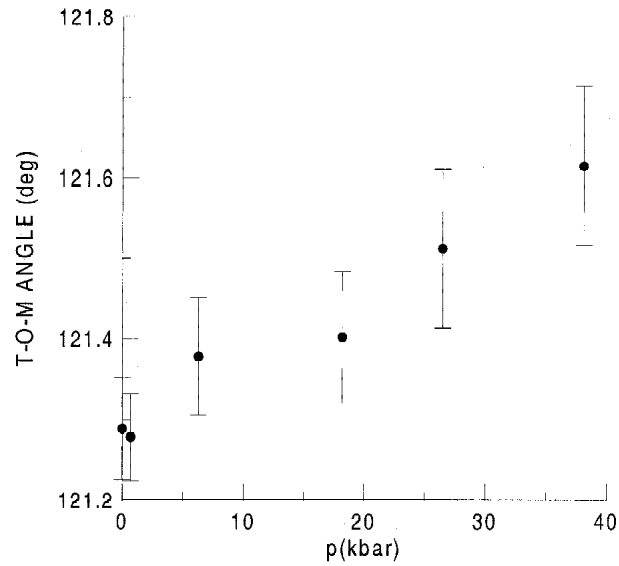

FIGURE 4. T-O-M angle (degrees) vs. pressure (kbar).

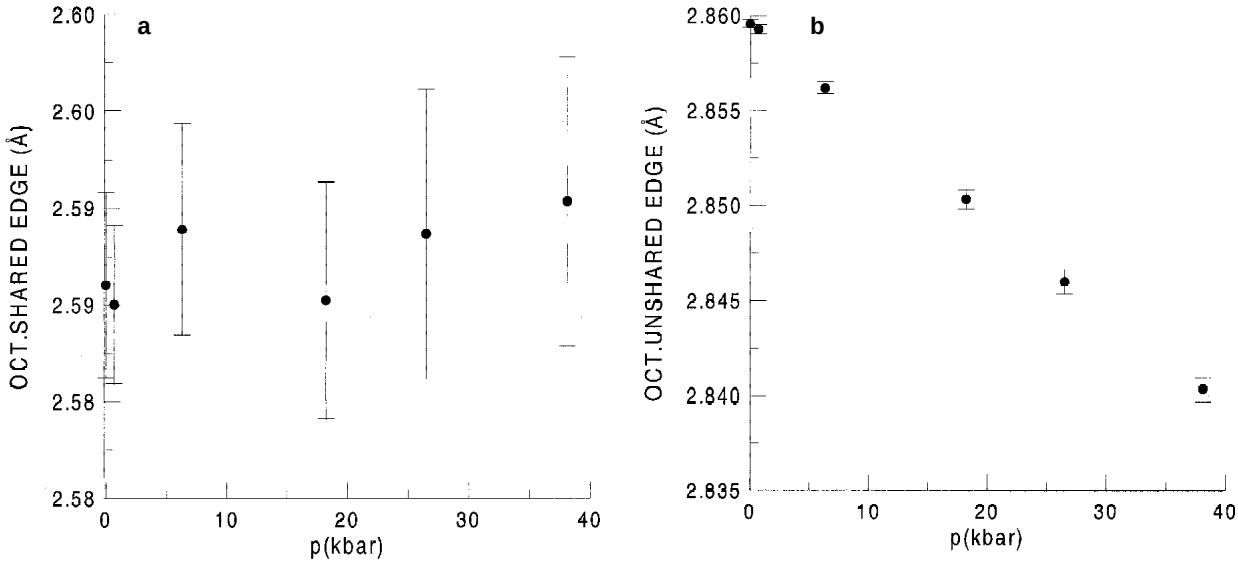

FIGURE 5. Shared **(a)** and unshared **(b)** octahedral edges (Å) vs. pressure (kbar).

T- or M-sites causes average weakening of the interactions, and consequent growing of the T-O-M angle compliance to pressure. Furthermore, the full dependence of the T-O-M angle on the oxygen *u*-coordinate, i.e., on the one positional degree of freedom of the spinel structure, indicates that this discrepancy is a consequence of the O-atom relaxation following the cation re-adjustment.

The rate of change of *te* and *oue* are –0.0011 Å/kbar (MRV = 344) and –0.0005 Å/kbar (MRV = 177), respectively, in agreement with the results from Finger et al. (1986). A marked stiffness is seen in *ose*, consistent with the change in a shared edge being more energy-demanding than modifying an unshared one, owing to the former structural rearrangement involving simultaneously two adjacent octahedra. The *te* interatomic distance exhibits the largest MRV value: The softness of this bond is related to the tetrahedral edge being significantly longer than it usually is in case of the Al/Si coordinated tetrahedra, and correspondingly it has a weaker O-O interaction.

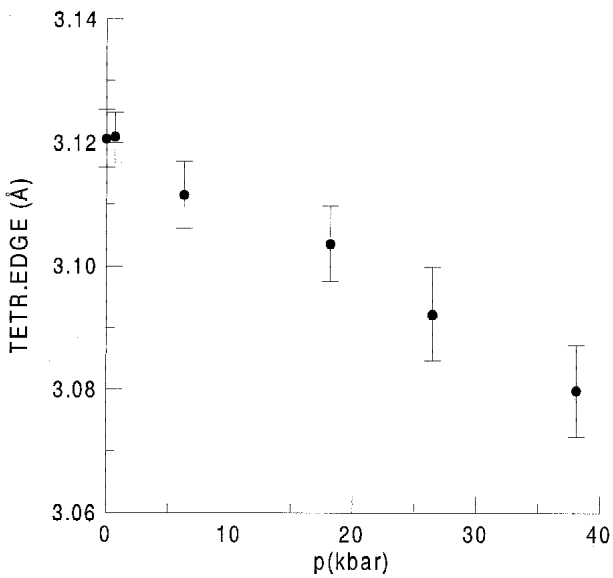

FIGURE 6. Tetrahedral edge (Å) vs. pressure (kbar).

The tetrahedral volume (V_T) (Fig. 7a) reduces by about –0.0036 Å/kbar (MRV = 1018), similarly to the results of Finger et al. (1986). However, the octahedral volume (V_M) vs. P (Fig. 7b) shows a distinct change at the OD-reaction pressure. The results of Finger et al. (1986) indicate V_M to behave similarly, with the shrinkage taking place between 30 and 40 kbar. The rate of variation we observe in V_M is about –0.0015 Å^3/kbar (MRV=160), as compared to a rate of –0.0030 Å^3/kbar from Finger et al. (1986). As a result, the M-site is significantly stiffer in our sample than it is in the natural specimen studied by Finger et al. (1986). Such a result is intuitively in contrast with the modest amount of vacancies in our synthetic sample, whose sensitivity to pressure ought thereby to increase. Possible explanations may involve (1) the presence of excess Al cations with respect to the ideal stoichiometry, (2) the occurrence of a cation rearrangement engendering structural relaxation by action of the modified force field, and (3) the compliance of the T-O-M angle.

Furthermore, in the present investigation the trend of the V_M/V_T ratio continuously increases from 2.62, at 1 atm, up to 2.71, at the highest pressure we explored; the same ratio calculated from the results of Finger et al. (1986) displays scattered values and a slightly increasing trend, ranging from 2.49 to 2.54. Given that the total volume occupied by octahedra and tetrahedra approximately corresponds to 34% of the cell volume, the behavior of V_M/V_T indicates that (1) at ambient pressure, our sample exhibits a smaller tetrahedral volume and a larger octahedral volume than that studied by Finger et al. (1986); this is consistent with a different starting site distribu-

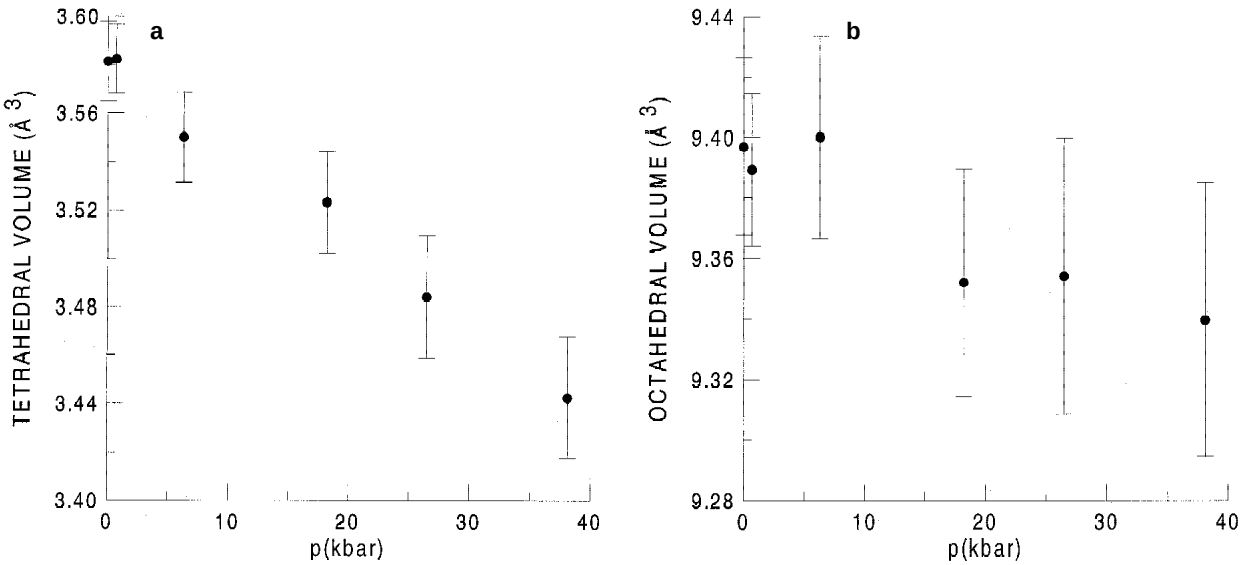

FIGURE 7. Tetrahedral **(a)** and octahedral **(b)** volumes (Å) vs. pressure (kbar).

tion of the cations. It is clear that our sample has some Mg at M-site; (2) both studies agree in indicating the tetrahedron to be softer than the octahedron; and (3) the significant increase of stiffness of the octahedron with respect to the tetrahedron in our sample is consistent with the migration of tetrahedrally coordinated aluminum to the M-sites.

Numerical simulations

The Gibbs free energy at the highest pressure achieved was calculated using the structural parameters we determined, and several possible cation distributions were tested. The potential energy model was limited to the Coulombic interactions, and other contributions were neglected. The evaluation of entropy was restricted to the configurational term, and vacancies were modeled as mere absence of charge, rather than being treated by more reliable approaches (Catlow and Mackrodt 1982). These calculations cannot yield absolute values for the system, but do provide adequate relative values for comparison among different cation configurations. Thus, the Gibbs free energies were calculated for various cation partitioning with respect to G ref determined from the structural data (atomic distribution, coordinates, and cell parameters) at room conditions. In kJ/mol, G-G ref = –191 for the partitioning derived in the present work; = –105 for partitioning obtained at ambient conditions; = –155 for Mg fully entering T-site and all vacancies either in M-sites; and = –203 kJ/mol for Mg in T-sites and all vacancies or in T-sites. Better stability is achieved by the model with the vacancies in the T-site. The energetic difference between our model and all vacancies and Mg in the T-site is very modest, and basically we cannot discriminate between them in the limits of the computational model. However, the suggestion is doubtless in favor of a cation arrangement tending toward a normal structure, with vacancies over the T-sites. The results of the simulations are consistent with the proposed interpretation of the structure as resulting from the diffraction study.

Natural Al-Mg-Fe spinels tend to have normal structures (e.g., Della Giusta et al. 1996), with Mg and Al cations ordered in T- and M-sites, respectively. From the above discussion, this is not a sole consequence of the cation rearrangement owing to slow cooling, but a P vs. T competitive action exerted at formation. These effects should be taken into account when interpreting the thermobaric history of spinels from cation partitioning data.

ACKNOWLEDGMENTS

The work was financially supported by Italian MURST and CNR. The authors are indebted to R. Angel, A. Della Giusta, A. Navrotsky, and J. Parise for critical read and suggestions, which greatly improved the manuscript. The anonymous referees are acknowledged for observations that much contributed to clarifying the text. A.P. is grateful to the "Centro di studio per la dinamica alpina e quaternaria" (CNR, Milan) for computational and chemical analysis facilities. The synthetic spinel sample was kindly supplied by M. Valle (ICRA, Bergamo, Italy). Neutron beamtime from Rutherford Appleton Laboratory is acknowledged.

REFERENCES CITED

Askarpour, V., Manghnani, M.H., Fassbender, S., and Yoneda, A. (1993) Elasticity of single-crystal $MgAl_2O_4$ spinel up to 1273 K by Brillouin spectroscopy. Physics and Chemistry of Minerals, 19, 511–519.

Birch, F. (1986) Equation of state and thermodynamic parameters on NaCl to 300 kbar in the high temperature domain. Journal of Geophysical Research, 91, 4949–4954.

Besson, J.M., Nelmes, R.J., Hamel, G., Loveday, J.S., Weill, G., and Hull, S. (1992) Neutron powder diffraction above 10 GPa. Physica B, 180 and 181, 907–910.

Carbonin, S., Russo, U., and Della Giusta, A. (1996) Cation distribution in some natural spinels from X-ray diffraction and Mössbauer spectroscopy. Mineralogical Magazine, 60, 355–368.

Catlow, C.R.A. and Mackrodt, W.C. (1982) Theory of simulation methods for lattice and defect energy calculations in crystal. In C.R.A. Catlow and W.C. Mackrodt, Computer simulation of solids, p. 1–20. Springer Verlag, Berlin

Della Giusta, A. and Ottonello, C. (1993) Energy and long-order in simple spinels. Physics and Chemistry of Minerals, 20, 228–241.

Della Giusta, A., Carbonin, S., and Ottonello, G. (1996) Temperature dependent disorder in a natural Mg-Al-Fe^{2+}-Fe^{3+} spinel. Mineralogical Magazine, 60, 603–616.

Finger, L.W., Hazen, R.M., and Hofmeister, A.M. (1986) High pressure crystal chemistry of spinel ($MgAl_2O_4$) and magnetite (Fe_3O_4): comparison with silicate spinels. Physics and Chemistry of Minerals, 13, 215–220.

Gasparik, T. and Newton, R.C. (1984) The reversed alumina contents of orthopyroxene in equilibrium with spinel and forsterite in the system MgO-

$A1_2O_3$-SiO_2. Contributions Mineralogy Petrology, 85, 186–196

Hazen, R.M. and Navrotsky, A. (1996) Effects of pressure on order-disorder reaction. American Mineralogist, 81, 1021–1035.

Hull, S., Smith, R.I., David, W.I.F., Hannon, A.C., Mayers, J., and Cywinski, R. (1992) The Polaris powder diffractometer at ISIS. Physica B, 180 and 181, l000–1002.

James, F. and Roos, M. (1975) Minuit-A system for function minimization and analysis of the parameter errors and correlations. Computational Physics Communications, 10, 343–367.

Larson, A.C, Von Dreele, R.B. (1987) GSAS: General Structure Analysis System. Los Alamos National Laboratory, Report LAUR: 86–87

Larsson, L. (1995) Temperature dependent cation distribution in a natural $Mg_{0.4}Fe_{0.6}A1_2O_4$ spinel. Neues Jahrbuch für Mineralogie Monatshefte, 4, 173–183.

Liu, L.G. (1975) Disproportionation of $MgAl_2O_4$ spinel at high pressure and temperatures. Geophysical Research Letters, 2, 9–11.

—— (1978) A new high pressure phase of spinel. Earth Planetary Science Letters, 41, 398–404.

—— (1980) The equilibrium boundary of spinel-corundum+periclase: a calibration curve for pressures above 100 kbar. High Temperatures-High Pressures, 12, 217–220.

Lucchesi, S. and Della Giusta, N. (1994) Crystal chemistry of non-stoichiometric Mg-Al synthetic spinels. Zeitschrift für Kristallographie, 209, 714–719.

Menegazzo, G., Carbonin, S., and Della Giusta, A. (1997) Cation and vacancy distribution in an artificially oxidized natural spinel. Mineralogical Magazine, 61, 411–421.

Millard, R.L., Peterson, RC., and Hunter, B.K. (1992) Temperature dependence of cation disorder in $MgAl_2O_4$ spinel, using ^{27}Al and ^{17}O magic-angle spinning NMR. American Mineralogy, 77, 44–52.

Nakagiri, N., Manghnani, M.H., Ming, L.C., and Kimura, S. (1986) Crystal structure of magnesite under pressure. Physics Chemistry of Minerals, 13, 238–244.

O'Neill, H.St.C. (1992) Temperature dependence of the cation distribution in zinc ferrite ($ZnFe_2O_4$) from powder XRD structural refinements. European Journal of Mineralogy, 4, 571–580.

O'Neill, H.St.C., Dollase, W.A., and Ross, C.R. (1991) Temperature dependence of the cation distribution in nickel aluminate ($NiAl_2O_4$) spinel: a powder XRD study. Physics and Chemistry of Minerals, 18, 302–319.

O'Neill, H.St.C., Annersten, H., and Virgo, D. (1992) The temperature dependence of the cation distribution in magnesioferrite ($MgFe_2O_4$) from powder XRD structural refinements and Mössbauer spectroscopy. American Mineralogist, 77, 725–740.

Pavese, A., Artioli, G., Russo, U., and Hoser, A. (1999) Cation partitioning versus temperature in $(Mg_{0.70}Fe_{0.23})Al_{1.97}O_4$ synthetic spinel, by in situ neutron powder diffraction. Physics and Chemistry of Minerals, in press.

Peterson, R.C., Lager, G.A., and Hitterman, R. (1991) A time-of-flight neutron powder diffraction study of $MgAl_2O_4$ at temperatures up to 1273 K. American Mineralogist, 76, 1455–1458.

Sack, R.O. and Ghiorso, M.S. (1991) Chromian spinels as petrogenetic indicators: thermodynamics and petrological applications. American Mineralogist, 76, 827–847.

Smith, R.I. and Hull, S. (1997) User guide for the Polaris Powder Diffractometer at ISIS. Rutherford Appleton Laboratory Report. RAL-TR-97, 38.

Viertel, H.U. and Seifert, F. (1979) Thermal stability of defect spinels in the system $MgAl_2O_4$-$A1_2O_3$. Neues Jahrbuch für Mineralogie Abhandlungen, 134, 167–182.

Wang, H. and Simmons, G. (1972) Elasticity of some mantle crystal structures 1. Pleonaste and hercynite spinel. Journal of Geophysical Research, 77, 4379–4392.

Wood, BJ., Kirkpatrick, R.J., and Montez, B. (1986) Order-disorder phenomena in $MgAl_2O_4$ spinel. American Mineralogist, 71, 999–1006.

Yamanaka, T. and Takeuchi, Y. (1983) Order-disorder transition in $MgAl_2O_4$ spinel at high temperatures up to 1700 °C. Zeitschrift für Kristallographie, 165, 65–78.

Yutani, M., Yagi, T., Yusa, H., and Irifune, T. (1997) Compressibility of calcium ferrite-type $MgAl_2O_4$. Physics and Chemistry of Minerals, 24, 340–344.

MANUSCRIPT RECEIVED JULY 23, 1998
MANUSCRIPT ACCEPTED DECEMBER 23, 1998
PAPER HANDLED BY JAMES W. DOWNS